

## Supplementary Materials for

### **Rapid identification of health care–associated infections with an integrated fluorescence anisotropy system**

Ki Soo Park, Chen-Han Huang, Kyunghoon Lee, Yeong-Eun Yoo, Cesar M. Castro, Ralph Weissleder, Hakho Lee

Published 6 May 2016, *Sci. Adv.* **2**, e1600300 (2016)  
DOI: 10.1126/sciadv.1600300

#### **The PDF file includes:**

- table S1. Target sequences recognized by established detection keys.
- table S2. Summary of a set of ARV factors targeted in this study.
- table S3. DNA sequences used in this study.
- fig. S1. Schematic of the plastic cartridge for RNA extraction.
- fig. S2. Comparison between the fluidic cartridge and a commercial column.
- fig. S3. The optical detection system in the PAD.
- fig. S4. Snapshots of a PAD application.
- fig. S5. The circuit diagram of the detection system.
- fig. S6. The effect of dUTP on the PAD assay.
- fig. S7. Portable PAD system.
- fig. S8. Lyophilized probes.
- fig. S9. Electrophoretic band-shift assay.
- fig. S10. Detection of ARV factors.
- fig. S11. Overall assay procedure for clinical samples.
- fig. S12. Universal and species-specific detection of HAI pathogens in clinical samples by the PAD system.
- fig. S13. Detection of ARV factors in clinical samples with PAD (top) and qPCR (bottom).
- References (29, 30)

**table S1.** Target sequences recognized by established detection keys.

Category	Target	DNA sequence (5' - 3')
Gram-positive	<i>Streptococcus</i>	GAAGAACGAGTGTGAGAGTGGAAAGTTCACACTGTGACGGTATCTTACCAGAAA GGGACGGCTAACTA
	<i>Enterococcus</i>	GAAGAACAAGGACGTTAGTAACTGAACGTCCCCTGACGGTATCTAACCAGAAAAG CCACGGCTAACTAC
	<i>Clostridium</i>	GTCTTCAGGGACGATAATGACGGTACCTGAGGAGGAAGCCACGGCTAACTACG TGCCAGCAGCCGCGGTAAT
	<i>Lactobacillus</i>	GGAGGCAGCAGTAGGGAATCTCCACAATGGACGCAAGTCTGATGGAGCAA
	<i>Corynebacterium</i>	CCTTTCGCAACCGACGAAGCTTTTGTGACGGTAGGTTGAGAAGAAGCACCGGC TAACT
	<i>Bacillus</i>	GTTGTTAGGGAGAACAAGTGC GTTCAAATAGGGCGGCACCTTGACGGTACCT AACCAGAAAAGCCACGG
Gram-negative	<i>Haemophilus</i>	TCATGGCATGCGGCCTTGCGGTCCC GCACTTTCATCTTCCGATTCTACGCGGTA TTAGCGAC
	<i>Proteus</i>	GGAGGAAGGTGATAAGGTTAATACCTTNTCAATTGACGTTACCCGCAGAAGAA GCACCGGCTAACTCC
	<i>Citrobacter</i>	ACGGAGTTAGCCGGTGCTTCTTCTGCGAGTAACGTCAATTGCTGCGGTTATTAA CCACAACACCTTCTCC
	<i>Serratia</i>	TCAGCGGGGAGGAAGGTGGTGAACCTAATACGTTCAATTGACGTTACTCGC AGAAGAAGCACCGGCTAA
	<i>Stenotrophomonas</i>	AATGCGTAGAGATCAGGAGGAACATCCATGGCGAAGGCAGCTACCTGGACCAA CATTGA
	<i>Legionella</i>	TTCAGTGGGGAGGAGGATTGATAGGTTAAGAGCTGATTGATTGGACGTTACCCA CAGAAGAAGCACCGGCT
	<i>Neisseria</i>	TTTGTCAGGGAAAGAAAAGGCTGTTGCTAATATCAGCGGCTGATGACGGTACCTG AAGAATAAGCACCGGCTA
	<i>Moraxella</i>	TTAAGTGGGGAGGAAAAGCTTGTGGTTAATACCCACAAGCCCTGACGTTACCCA CAGAATAAGCA
	<i>Bacteroides</i>	TCATTAGACATAAAGTGCAGTCATGTCATGTCATACTGTTTTGTCATGTCATAATA TGAATAAGGATCGGCT
	<i>Mycobacterium</i>	TCTTTCACCATCGACGAAGGTCCGGGTTCTCTGGATTGACGGTAGGTGGAGAA GAAGCACCGGCCAA

**table S1 (continued).** Target sequences recognized by established detection keys.

Gene	Protein name	DNA sequence (5' - 3')
ramA	Transcriptional activator	TACCGACCAGCGGGTTTATGATATCTGCCTGAAATACGGCTTTGATTTCGCAGCAGAC
KPC	Carbapenem-hydrolyzing beta-lactamase	CGGCATAGTCATTTGCCGTGCCATACCCTCCGCAGGTTCCGGTTTTGTCTCCGACTG
NDM	Beta-lactamase	CGCATTGGCATAAGTCGCAATCCCCGCCGCATGCAGCGCGTCCATACCGCCCATCTTGT
OXA	Beta-lactamase	ACCCAACCTGTAAACCAACCTACTTGAGGGGTACAGCCATCCCCAGCCGCTTTTTG
IMP	Beta-lactamase	TGAATATTTAGCTTGTACCTTACCGGATTTTTTCAAAGTTCATTTGTTAATTCAGAT
VIM	Beta-lactamase	TAGCCGAGGTAGAGGGGAACGAGATTCCCACGCACTCTCTAGAAGGACTCTCATCGAGCG G
SPM	Beta-lactamase	CGTTAAATGCACGGTTGGGGATGTGAGACTACAGTCTCATTTGCGCAACGGCCTTTTC
CTX-M	Beta-lactamase	CGTTAAACACCGCCATTCCGGGCGATCCGCGTGATACCACTTCACCTCGGGC
TEM	Beta-lactamase	TTGCACAACATGGGGGATCATGTAACCTCGCCTTGATCGTTGGGAACCGGAGCTGAATGAA
ampC	Beta-lactamase	GCGTCAAATCGACACTACCCGACATGTTGAGTTTTATT CATGCCAACCTTAACCCACAGA
vanA	Vancomycin/teicoplanin A-type resistance	TCCAATTCGTCCGCGCTATTGACTTTTTTACACCGAAGGATGAGCCTGAAC

**table S2.** Summary of a set of ARV factors targeted in this study (19, 20, 29, 30).

Gene	Protein name	Function	Positive strain
<i>nuc</i>	Thermonuclease	<i>S. aureus</i> specific factor important for in vivo survival	HA-MRSA (ATCC BAA-1720), CA-MRSA (ATCC BAA-1707), MSSA (ATCC 25923)
<i>femB</i>	Aminoacyltransferase	<i>S. aureus</i> specific factor essential for methicillin resistance, affecting level of resistance	HA-MRSA (ATCC BAA-1720), CA-MRSA (ATCC BAA-1707), MSSA (ATCC 25923)
<i>mecA</i>	Penicillin binding protein 2A	Methicillin resistance determinant	HA-MRSA (ATCC BAA-1720), CA-MRSA (ATCC BAA-707)
PVL	Panton-Valentine Leukocidin	A cytotoxin, one of the $\beta$ -pore-forming toxins, affecting virulence of <i>S. aureus</i>	CA-MRSA (ATCC BAA-1707), MSSA (ATCC 25923)

**table S3.** DNA sequences used in this study.

Target	Strand name	DNA sequence (5' - 3')	
Universal	Amplicon	GGTAAGGTTCTTCGCGTTGCN*TCGAATTAACCACATGCTCCA	
	Limiting primer	GGAGCATGTGGTTTAATTCGA	
	Excess primer	GGTAAGGTTCTTCGCGTT	
Reporter	Template	CATGAATCTACTCGACGATATTGCTCAACTGTCATAAACTTCTGAGGA	
	Primer	TCCTCAGAAGTTT	
	FAM-DNA	(FAM)-TATCGTCGAGTAGATTCATG	
Species differentiation	<i>Escherichia</i>	Amplicon	TGCGGGTAACGTCAATGAGCAAAGGTATTAACCTTACTCCCTCCTCCA
		Limiting primer	GGAGGAAGGGAGTAAAGTTAATACCTTTG
		Excess primer	TGCGGGTAACGTCAATGAG
	<i>Klebsiella</i>	Amplicon	ACGGCAGTTAGCCGGTGCTTCTTCTGCGGGTAACGTCCAATCGCCAAGGTTATT AACCTTATCGCCTTGCCTCCA
		Limiting primer	GGAGGCAAGGCGATAAGGT
		Excess primer	ACGGCAGTTAGCCGGTGCTTCT
	<i>Acinetobacter</i>	Amplicon	GAGTTAGCCGGTGCTTATTCTGCGAGTAACGTCCACTATCCCTAGGTATTA ACTA GAA
		Limiting primer	TCTAGTTAATACCTAGGGATAGTGGACGTT
		Excess primer	GAGTTAGCCGGTGCTTATTCTGCGAG
	<i>Pseudomonas</i>	Amplicon	TATTCTGTTGGTAACGTCAAAACAGCAAGGTATTAACCTACTGCCCTCCTCCA
		Limiting primer	GGAGGAAGGGCAGTAAGTTAATACCTTG
		Excess primer	GCTTATTCTGTTGGTAACGTCAAAACAG
	<i>Staphylococcus</i>	Amplicon	GTAGTTAGCCGTGGCTTTCTGATTAGGTACCGTCAAGATGTGCACAGTTACTTA CACATATGTTCTTCCCA
		Limiting primer	GGGAAGAACATATGTGTAAGTAAC
		Excess primer	GTAGTTAGCCGTGGCTTTCT
Resistance and virulence	<i>nuc</i>	Amplicon	CACCTGAAACAAAGCATCCTAAAAAAGGTGTAGAGAAATATGGTCCTGAAGCAA
		Limiting primer	TGCTTCAGGACCATATTTCTCTAC
		Excess primer	CACCTGAAACAAAGCATCCTAAA
	<i>femB</i>	Amplicon	TGAATTGAGCAAAACGGACGGCCCAATTCTAAACCTTGCTTCTGGA
		Limiting primer	CCAGAAGCAAGGTTTAGAATTG
		Excess primer	TGAATTGAGCAAAACGGACGGC
	<i>mecA</i>	Amplicon	ATGAAGGTGTGCTTACAAGTGCTAATAATTACCTGTTTGAGGGTGGATAGCAGA
		Limiting primer	CTGCTATCCACCCTCAAACAGG
		Excess primer	ATGAAGGTGTGCTTACAAGTGC
	PVL	Amplicon	CACCTGATAAGCCGTTAGAGATATTAATATCTCCACCATAAGAATAACCTACCGA
		Limiting primer	CGGTAGGTTATTCTTATGGTGGAGAT
		Excess primer	CACCTGATAAGCCGTTAGAGATATT

\* The nucleobase in bold letter (N) indicates Adenine (A) for *Escherichia*, *Klebsiella*, *Acinetobacter* or Thymine (T) for *Pseudomonas*, *Staphylococcus*.

## Supplementary Figures

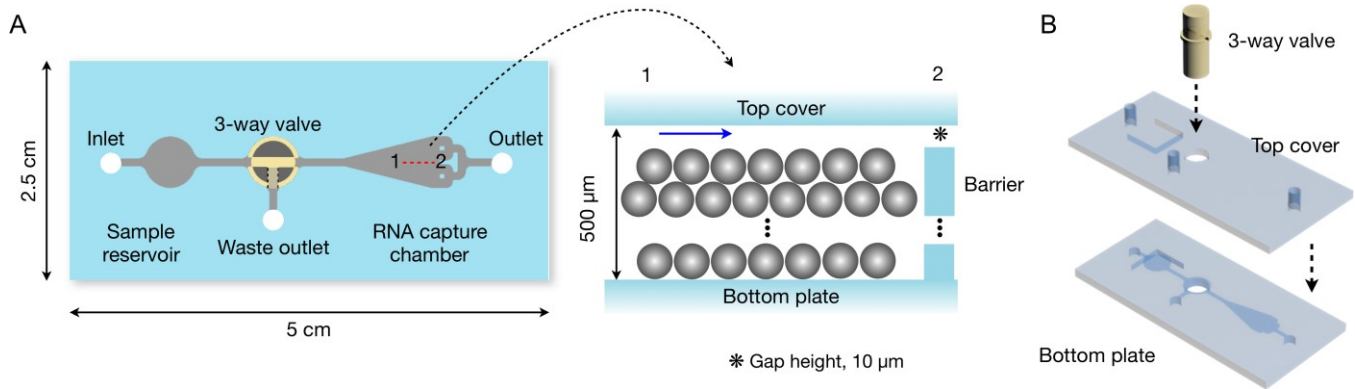


**fig. S1. Schematic of the plastic cartridge for RNA extraction. (A)** Top view. The device has a RNA capture chamber that is filled with glass beads. The 3-way valve (push-button style) is used to direct waste product to a separate outlet. The RNA chamber has weir style barrier (right) to retain glass beads while allowing for fluidic flow. Gap height (\*), 10 μm. **(B)** Device assembly. The bottom plate and the top cover were separately injection-molded, and glued together.

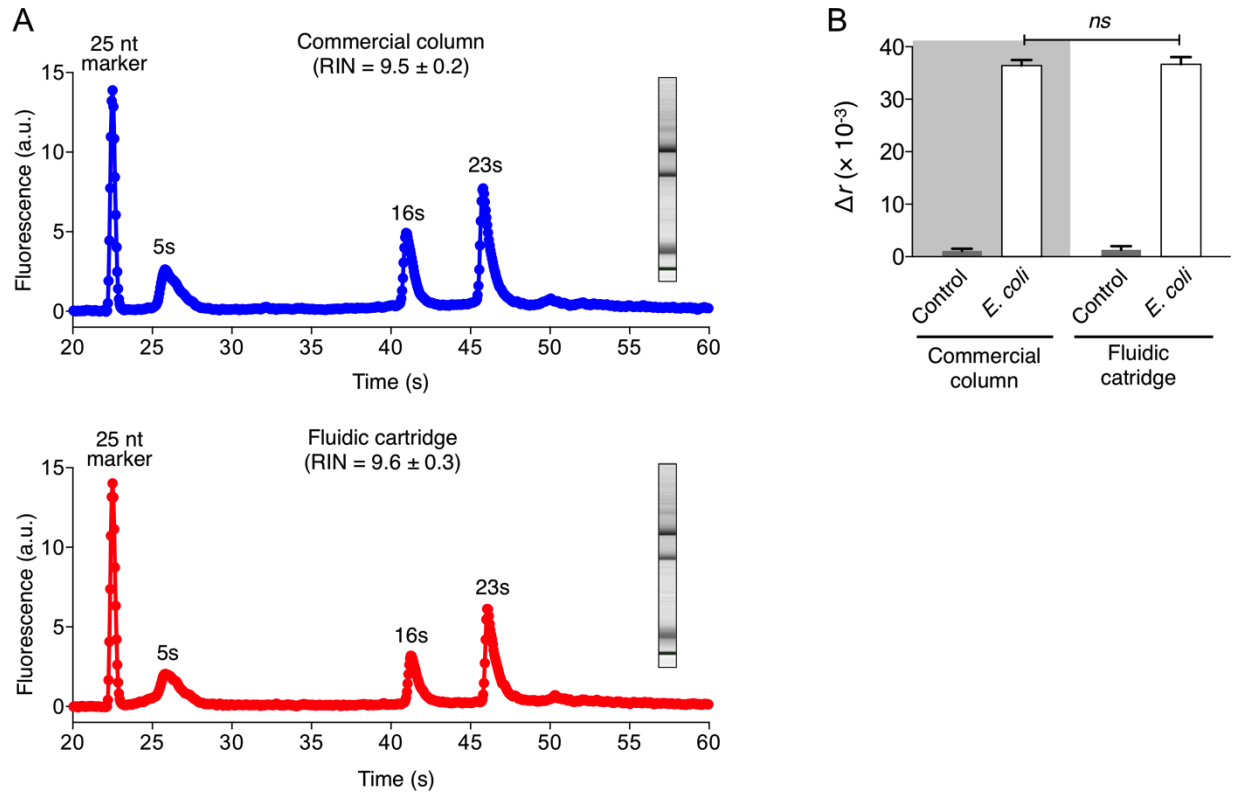


**fig. S2. Comparison between the fluidic cartridge and a commercial column.** Equal volumes of *E. coli* lysates were flown through a commercial column (Zymo Research) and the fluidic cartridge for total RNA extraction. **(A)** The RNA integrity was assessed by Bioanalyzer (Inset: ‘virtual gel’ pattern from the instrument). The RNA integrity number (RIN) indicated that high quality RNA was collected by the fluidic cartridge (RIN =  $9.6 \pm 0.3$ ). The number was comparable to that of a commercial column (RIN =  $9.5 \pm 0.2$ ). **(B)** The RNA extracted by a commercial column and the fluidic cartridge was amplified by asymmetric RT-PCR and detected by the PAD. The observed  $\Delta r$  values were statistically identical (two-tailed *t*-test,  $P > 0.64$ ).

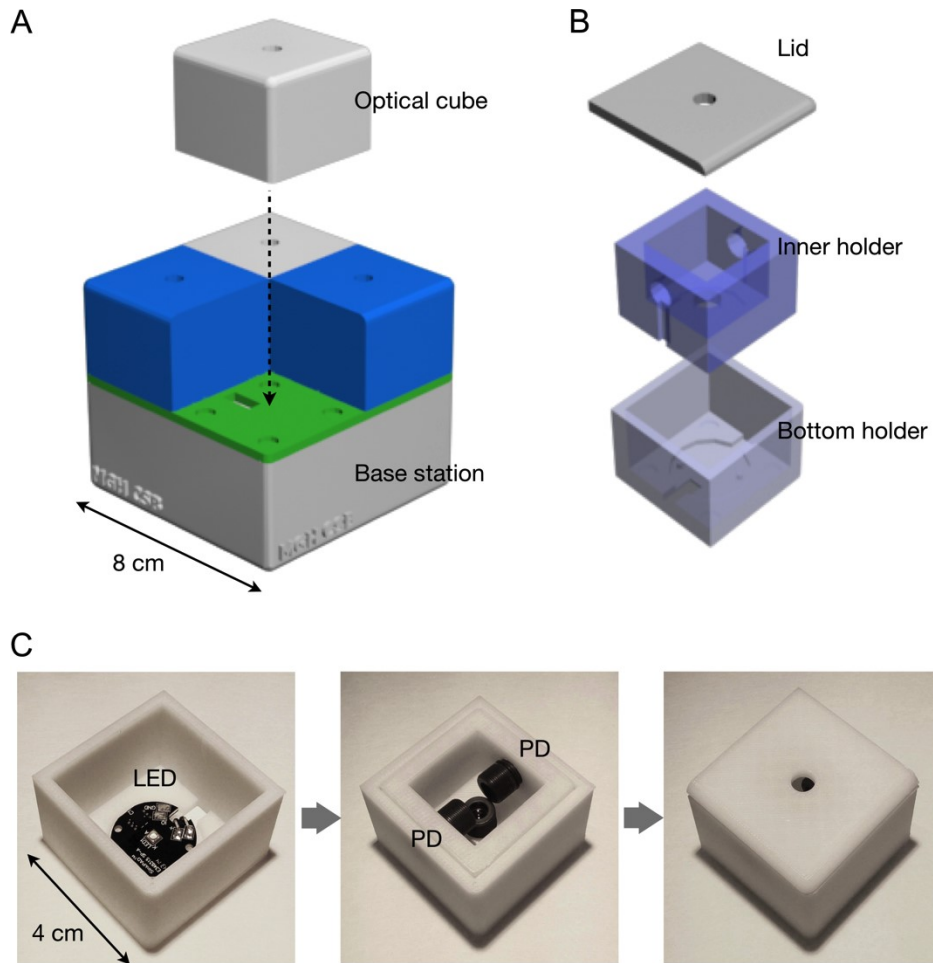


**fig. S3. The optical detection system in the PAD. (A)** The system has a modular structure. The base station contains control electronics, including a microcontroller and signal processing units. Four optical cubes are plugged into the base station. **(B)** Blow-up schematic of an optical cube. **(C)** Optical cube assembly. A LED circuit was positioned on the bottom holder. The inner holder, mounted with photodiodes (PDs), focusing lenses, and optical filters (polarizers), was inserted into the bottom holder and capped with a lid.



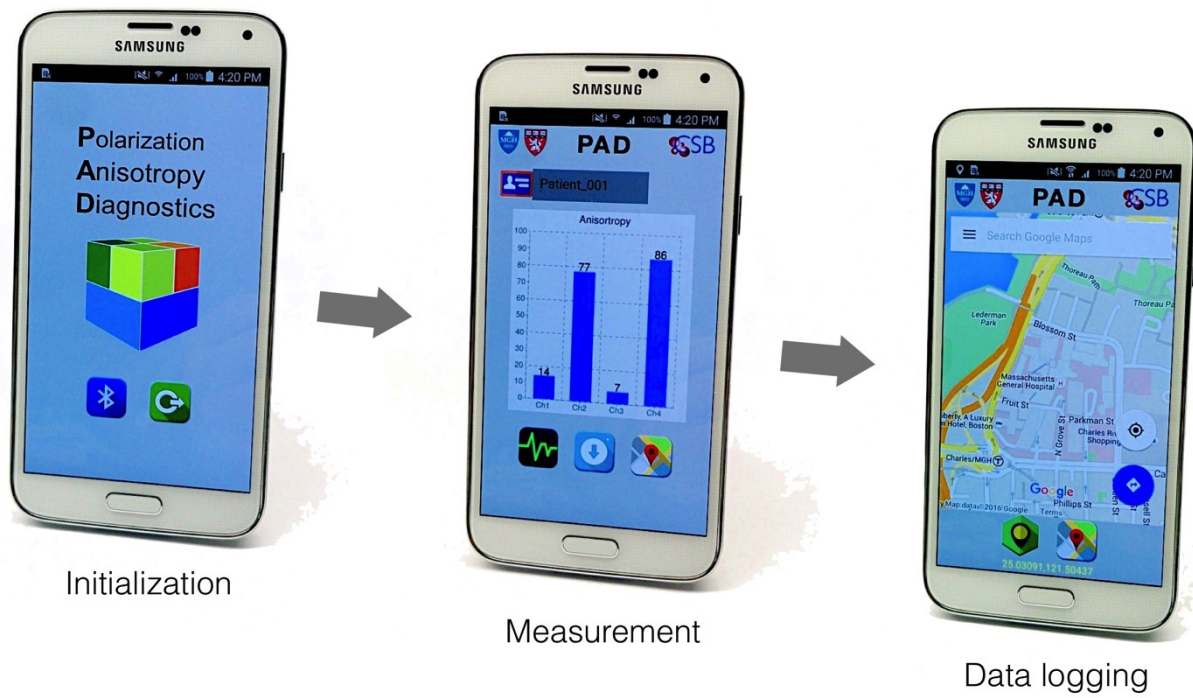


**fig. S4. Snapshots of a PAD application.** The PAD App has three main pages, namely, system initialization, measurement, and data storage with the geographic information.

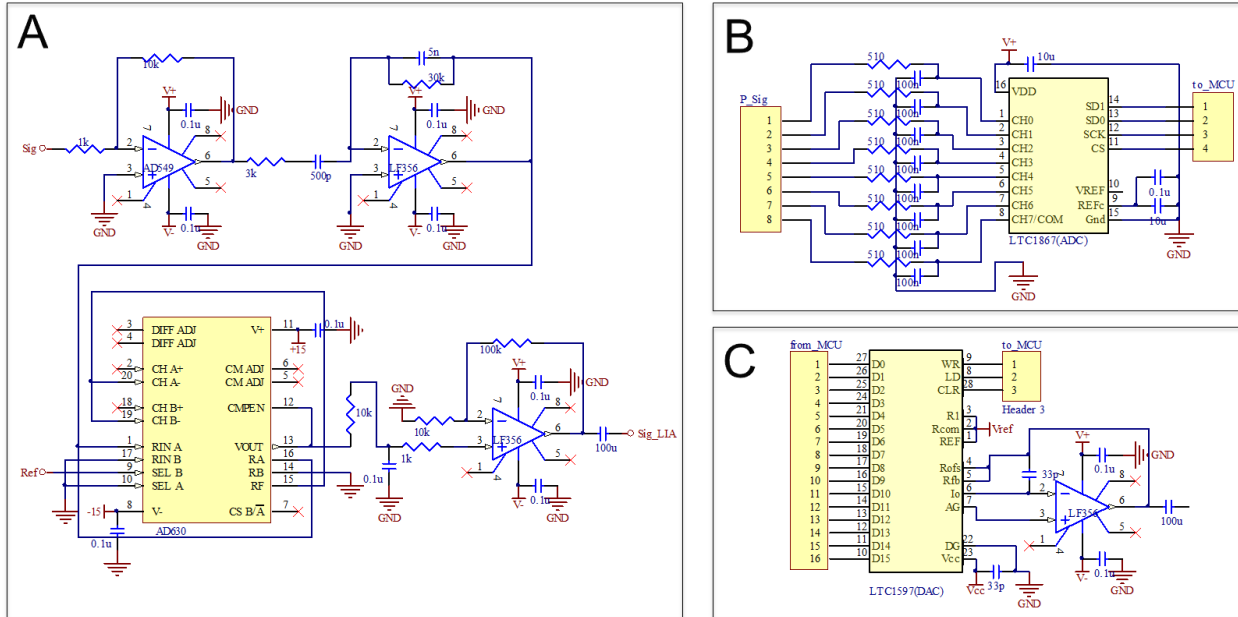


**fig. S5. Circuit diagrams of the detection system. (A)** Schematic of a custom-designed current amplifier circuit (AD549; Analog Devices), an active band pass filter, an analog lock-in circuit (AD630; Analog Devices), and a low pass filter. **(B)** A 16-bit analog-to-digital converter (LTC1867; Linear Technology) with a configurable 8-channel analog input multiplexer (MUX) was used. **(C)** A 16-bit digital-to-analog converter (LTC1597; Linear Technology) was used to deliver the modulated control signal to the LED driver.

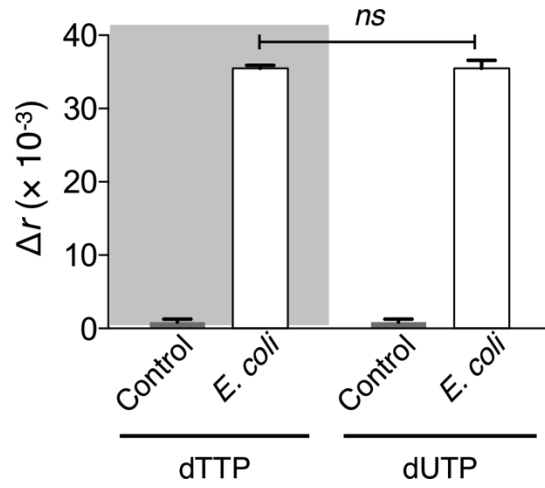


**fig. S6. The effect of dUTP on the PAD assay.** As compared to the original assay condition in which dTTP was used (left), no difference was observed when dTTP was replaced with dUTP (right). The observed  $\Delta r$  values in both cases were statistically identical (two-tailed *t*-test,  $P > 0.99$ ).

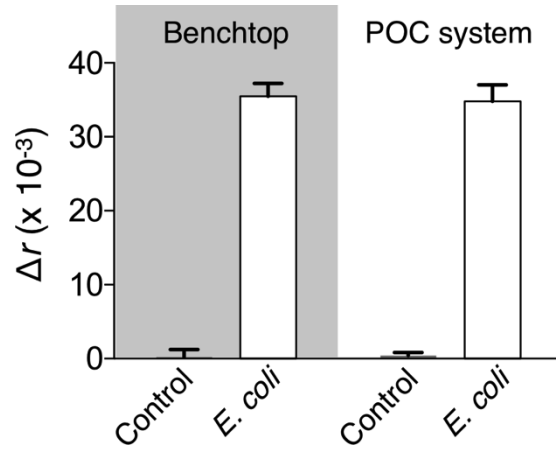


**fig. S7. Portable PAD system.** For on-site, point-of-care (POC) operation, the PAD detection was paired up with a miniaturized thermocycler (MiniPCR; Ampylus). The performance of a benchtop equipment and the POC-PAD was statistically identical (two-tailed *t*-test, *P* > 0.69).

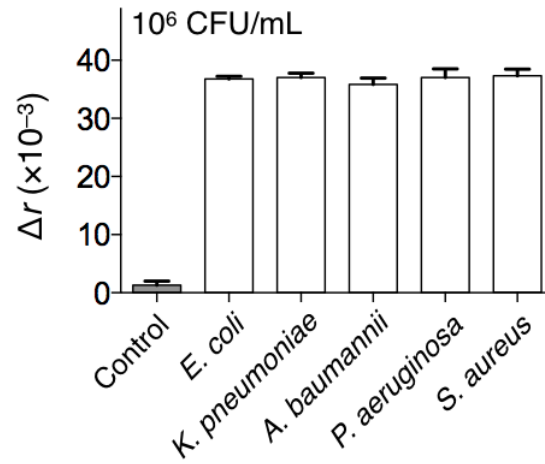


**fig. S8. Lyophilized probes.** The PAD reagents were lyophilized, stored for 2 weeks in ambient condition, and then used for bacterial detection. Five different HAI pathogens (10<sup>6</sup> CFU/mL) were detected with lyophilized reagents. The signal levels were comparable to those obtained by fresh reagents (**Fig. 3B**). All experiments were performed in triplicate, and the data are displayed as mean ± s.d.

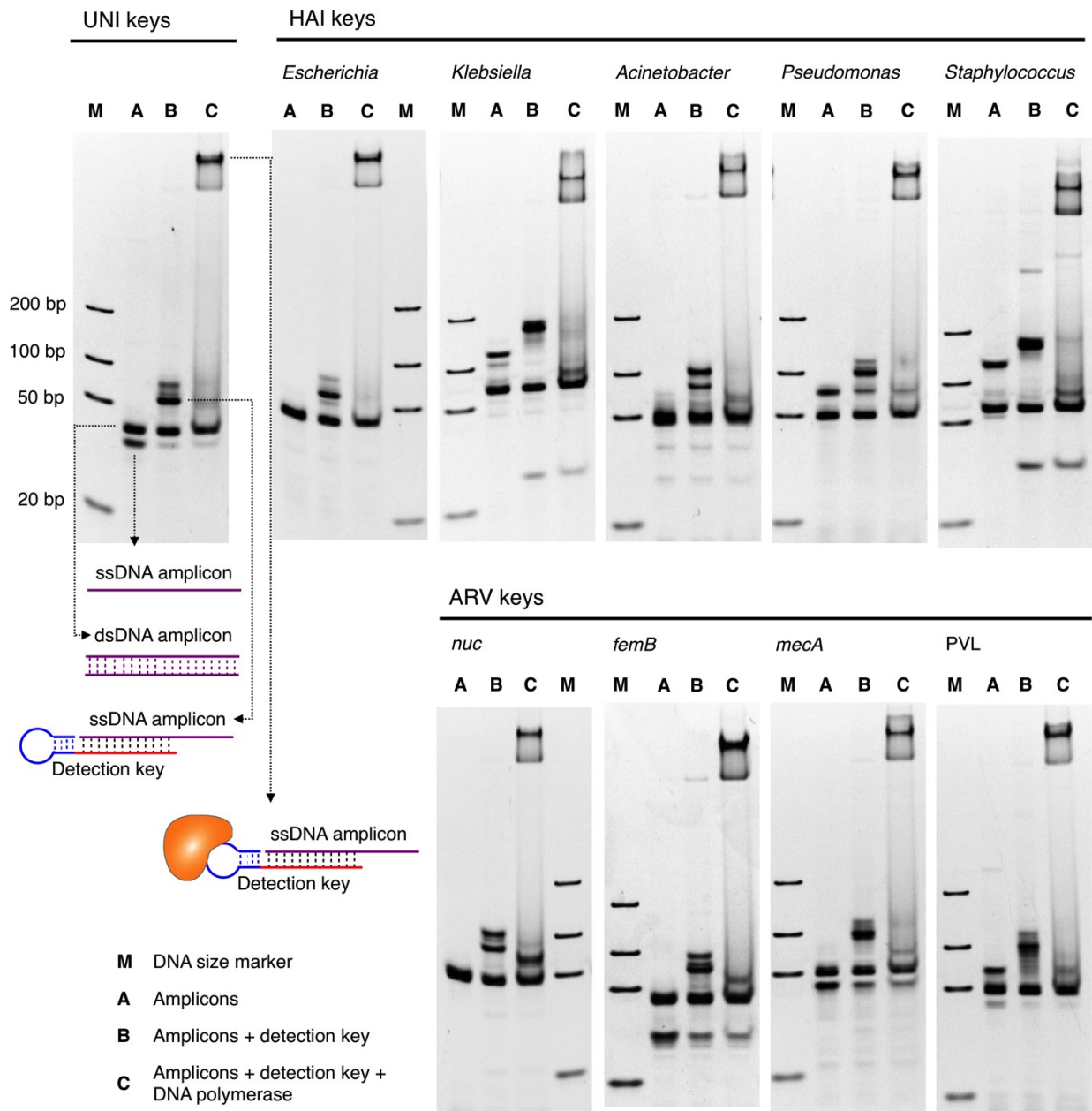


**fig. S9. Electrophoretic band-shift assay.** Lane A. Amplicons only. Lane B. Binding of amplicons with their detection keys produced new bands. Lane C. Adding DNA polymerase to B shifted the band for the amplicon and detection-key hybrid. This confirmed the binding between detection keys and DNA polymerase.

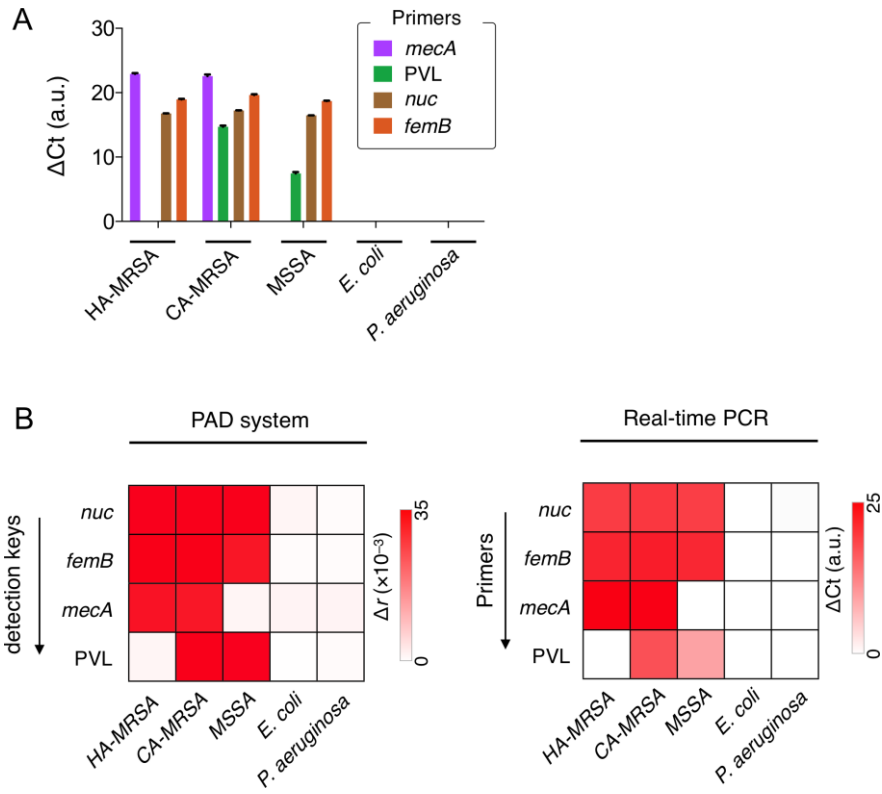


**fig. S10. Detection of ARV factors. (A)** Real-time PCR detection of *mecA*, PVL, *nuc*, and *femB* in bacterial species. SYBR Green assay was used. **(B)** Comparison between the PAD and the qPCR assays.

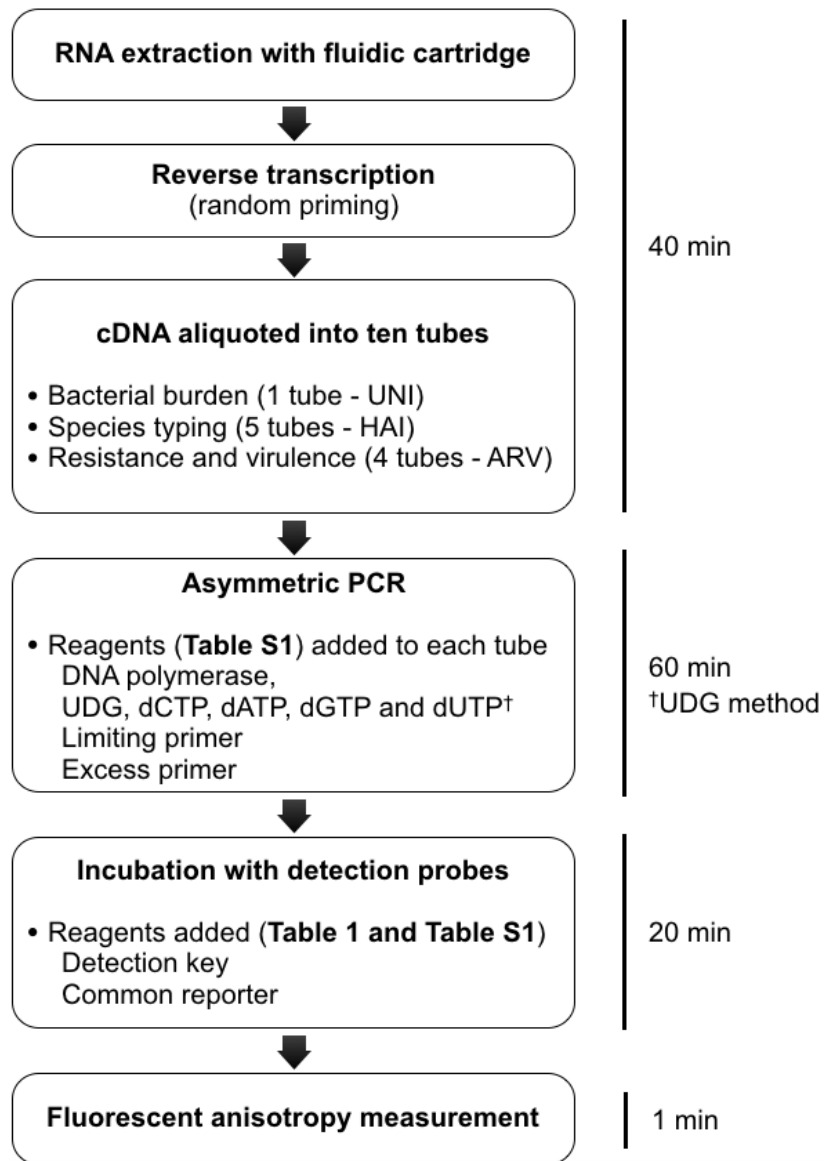


**fig. S11. Overall assay procedure for clinical samples.** Once the sample is aliquoted into individual tubes, the rest of the procedures are performed in the same tube.



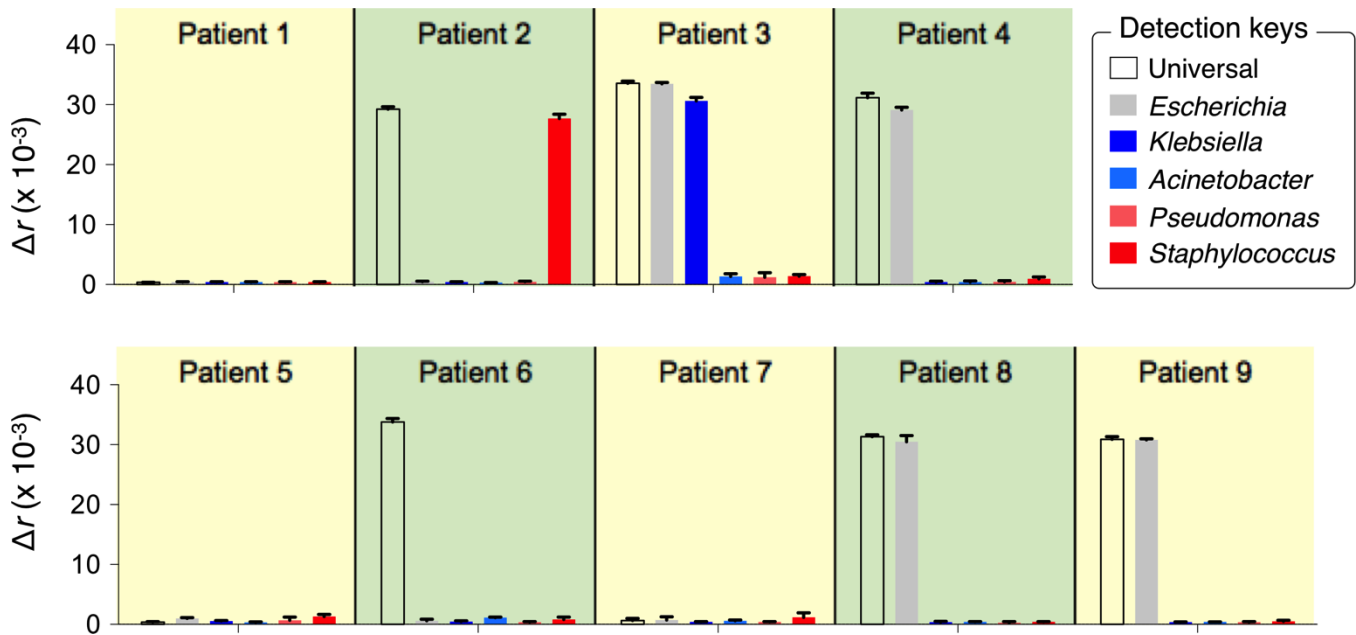


fig. S12. Universal and species-specific detection of HAI pathogens in clinical samples by the PAD system.

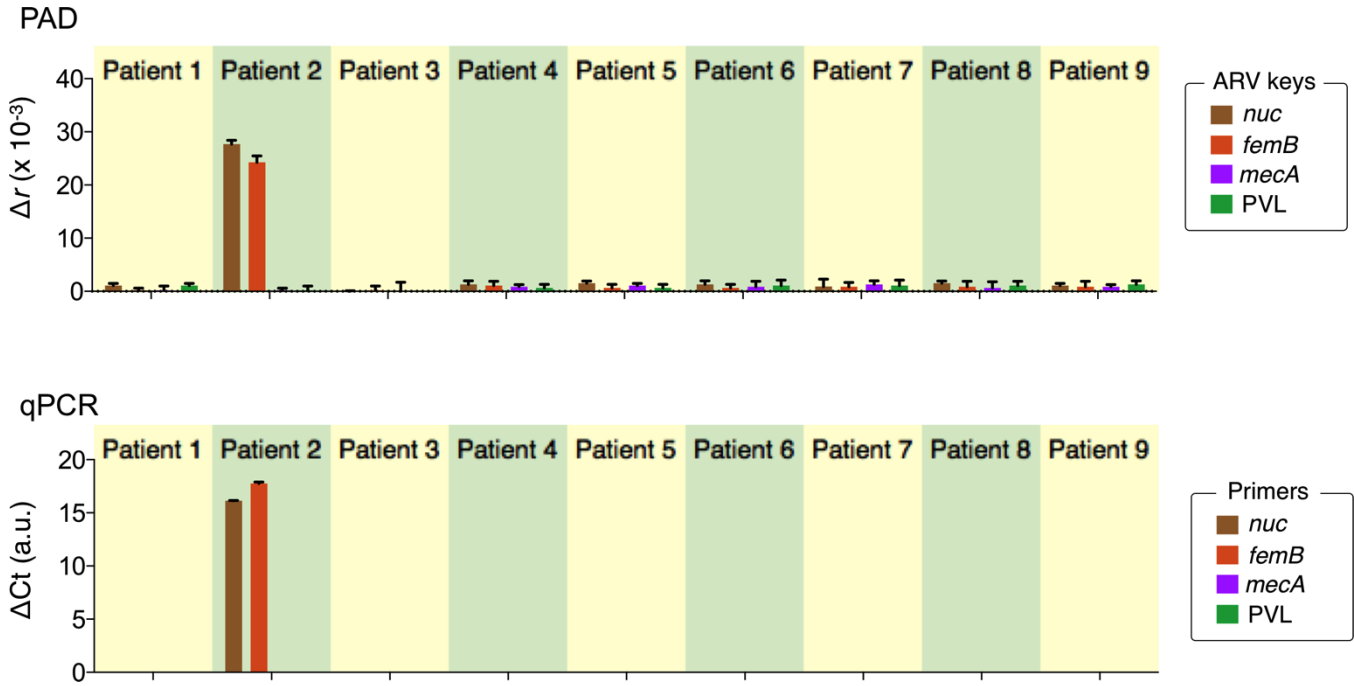


fig. S13. Detection of ARV factors in clinical samples with PAD (top) and qPCR (bottom).